

Supporting Information

Leveraging 3D Printing for the Design of High-Performance Venturi Microbubble Generators

Yirong Feng, Hongfeng Mu, Xi Liu, Zhengliang Huang, Haomiao Zhang*,
Jingdai Wang, and Yongrong Yang

State Key Laboratory of Chemical Engineering, College of Chemical and
Biological Engineering, Zhejiang University, Hangzhou 310027, PR China

*Corresponding author. E-mail address: haomiaozhang@zju.edu.cn

S1. Proof of Manufacturing Accuracy

As a standard approach, we pre-checked the dimensions of the 3D printed venturi structures since fabrication tolerances may lead to certain levels of manufacturing inaccuracy. Under this direction, we 3D printed venturi channels with designed divergent angles (α_{design}) of 5°, 10°, 15°, 20°, and 25° (Figure S1), as used in the experiments, and measured their dimensions to determine the measured divergent angles ($\alpha_{measured}$) using inverse trigonometric functions. The comparison is presented in Table S1, which shows very good accuracy with this technique to investigate venturi channel design at microscale.

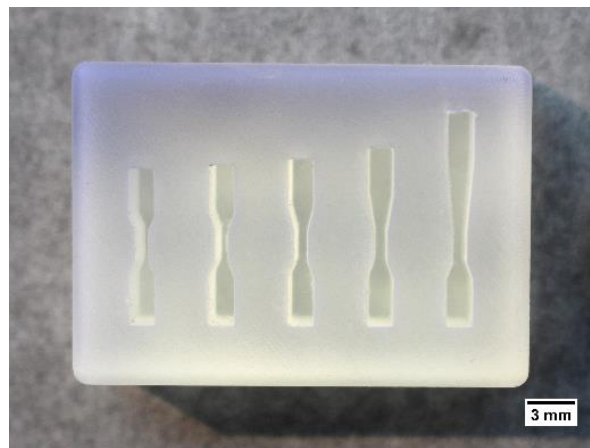


Figure S1. 3D printed five venturi structures with different divergent angles (from left to right: 5°, 10°, 15°, 20°, and 25°).

Table S1. Designed divergent angles (α_{design}) vs the measured ones ($\alpha_{measured}$).

α_{design}	$\alpha_{measured}$
5°	5.36°
10°	9.63°
15°	15.72°
20°	20.85°
25°	24.83°

S2. Proof of Solvent Compatibility

It is reported that Formlabs has measured resistance of resin “FLGPCL04” to solvents by observing, measuring, and weighing cured resin cubes (originally measuring 1 cm × 1 cm × 1 cm) before and after soaking in a solvent for 24 hours.¹ We also measured a few following the same procedure. Table S2 shows weight gain (%) by resin “FLGPCL04” after 24-hour exposure to selected solvents.

Table S2. Weight gain (%) by resin “FLGPCL04” after 24-hour exposure to solvents.

Solvent	Weight gain [%]	Reference
Ethanol	< 1.0	This work
Isopropyl alcohol	< 1.0	This work
Toluene	< 1.0	This work
Xylene	< 1.0	This work
Butyl acetate	< 1.0	(1)
Acetone	sample cracked	(1)
Strong acid (HCl conc)	distorted	(1)
Sodium hydroxide (0.025%, pH≈~10)	< 1.0	(1)

S3. CFD Simulation

We performed 2D axis-symmetric CFD simulation with COMSOL Multiphysics 5.3a to reveal the internal flow patterns, turbulence energy dissipation rate, and turbulence kinetic energy in the venturi channel at hydrodynamics steady-state. Due to the relatively small amount of the gaseous phase, we estimated the turbulence profiles using a single-phase simulation, which significantly saved

computational cost but provided enough accuracy. A liquid flow rate (Q_L) of 130 mL/min was employed as an illustration, corresponding to Re_{th} of 3,800. The so called “low Reynolds number $k - \epsilon$ turbulence model” in COMSOL was used to improve accuracy of wall functions, in which viscous effects dominate in the region close to the wall. The Navier-Stokes equation in conjunction with the continuity equation is solved at steady-state with boundary conditions applied corresponding to (i) inlet flowrate, (ii) outlet atmospheric pressure, (iii) no-slip wall, and (iv) axial symmetry. In this study, the grid size ranges from 0.016 μm to 0.0054 mm. In a ThinkPad P50 Workstation with Intel Core i7-6820HQ CPU @ 2.70 GHz, and 64 GB RAM, each stationary simulation takes 1-2 hours.

Figure S2 illustrates 2D maps of the steady-state turbulence energy dissipation rate (ϵ) at five different divergent angles (α). The maximum turbulence energy dissipation rate (ϵ_{max}) is found to be higher at larger α . As α increases, the corresponding location where ϵ_{max} appears is closer to the inlet of diverging section, suggesting a severer impact at higher α .

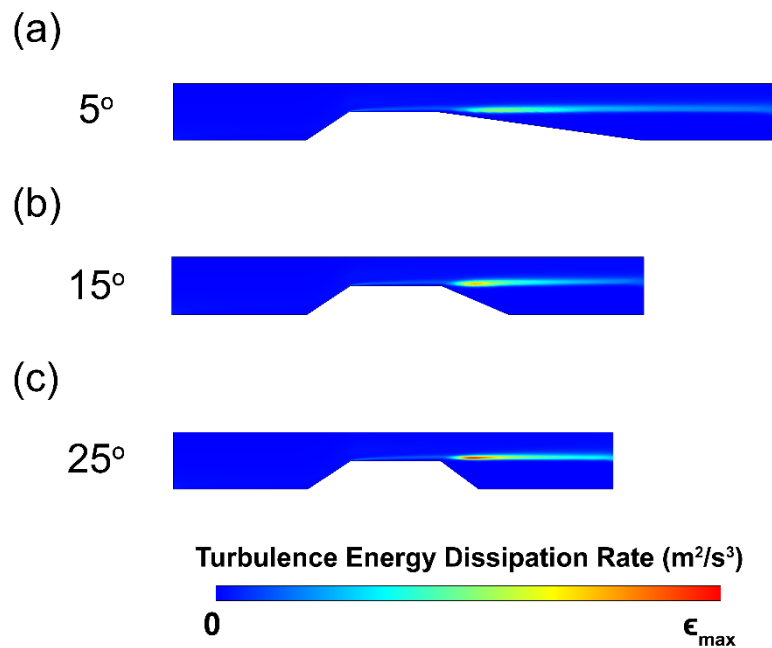


Figure S2. Steady-state turbulence energy dissipation rate (ϵ) vs divergent

angle (α) of (a) 5°, (b) 15°, and (c) 25°. For visual clarification, the actual aspect ratio is not preserved.

S4. Specific Interfacial Area

After the specific interfacial area (a) per unit volume of the gas-liquid mixture (m^2/m^3) is determined by Eq. 5, we obtained the corresponding predictive models under different experimental conditions as summarized in Table S3.

Table S3. Correlations of the gas-liquid interface area (a) with respect to gas holdup (ε_G) under different divergent angles ($\alpha = 5 - 25$), $\varepsilon_G = 0.02 - 0.16$, and $Re_{th} = 2400 - 4700$.

α	Correlations
5°	$a = 270 \times Re_{th}^{0.423} \varepsilon_G^{0.846}$
10°	$a = 88.2 \times Re_{th}^{0.514} \varepsilon_G^{0.686}$
15°	$a = 93.9 \times Re_{th}^{0.514} \varepsilon_G^{0.669}$
20°	$a = 104 \times Re_{th}^{0.525} \varepsilon_G^{0.720}$
25°	$a = 84.8 \times Re_{th}^{0.556} \varepsilon_G^{0.727}$

Reference

(1) https://support.formlabs.com/s/article/Solvent-Compatibility?language=en_US